ScientificScholar®
Knowledge is power
Publisher of Scientific Journals

www.clinicalimagingscience.org

Journal of Clinical Imaging Science

Musculoskeletal Imaging *Pictorial Essay*

Chordoma at the skull base, spine, and sacrum: A pictorial essay

Sin Hang Lee[1], Kai Yan Kwok[1], Sin Man Wong[2], Chik Xing Jason Chan[1], Yu Ting Wong[1], Man Lung Tsang[1]

[1]Department of Radiology, Tuen Mun Hospital, Tuen Mun, [2]Department of Radiology, CUHK Medical Centre, Sha Tin, Hong Kong.

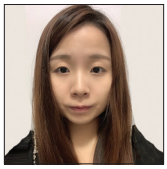

***Corresponding author:**
Sin Hang Lee,
Department of Radiology, Tuen Mun Hospital, Tuen Mun, Hong Kong.

sylviashlee0911@gmail.com

Received : 05 June 2022
Accepted : 10 July 2022
Published : 05 August 2022

DOI
10.25259/JCIS_62_2022

Quick Response Code:

ABSTRACT

Chordomas are rare tumors believed to be arising from the notochord remnant in the axial skeleton. Diagnosis is often difficult since they show overlapping imaging features with other more common disease including metastases. Since individualized papers are only discussing the imaging features at different locations, the aim of this pictorial review is to have a comprehensive review on the common imaging findings of chordomas along the entire neuroaxis with a series of pathological proven cases in a local tertiary hospital in Hong Kong.

Keywords: Chordoma, Skull base tumor, Sacral tumor, Vertebral body tumor

INTRODUCTION

Chordomas are rare tumors believed to be arising from the notochord remnant. They are usually found in the axial skeleton, including the clivus of the skull base, vertebral bodies of the mobile spine, and sacrococcygeal regions.

Chordomas commonly affect adults in their age of 60s. However, they could also be present in any age group. Diagnosis is often difficult since there are overlapping imaging features with other differential diagnoses including chondrosarcoma and metastasis. Biopsy may often be required for a definitive diagnosis.

This pictorial essay aims to illustrate the common imaging features of chordoma with a series of pathology-proven cases searched from the database of a local tertiary hospital in Hong Kong from 2008 to 2021.

EPIDEMIOLOGY

According to the recent descriptive epidemiology in the United States, the age-adjusted incidence rate of all types of chordomas was 0.88 per million persons per year from 2001 to 2014.[1] The annual age-standardized incidence rate of chordomas in Taiwan from 2003 to 2010 was 0.4 per million, showing male predominance.[2]

Chordomas commonly affect the adult population with a median age at diagnosis of 60 years.[3] There is a male predominance for all types of the chordomas in the adult group.[4] Cranial chordomas are the most common type, accounting for 38.7% of all types of chordomas followed by the sacral type (34.3%) and spinal type (27.0%).[1] Cranial chordomas occurred more

in the Asian/Pacific individuals, whereas the incidences of spinal and sacral chordomas were highest in the Caucasians population.[4]

Chordomas could also affect the children and young adult's populations. There is a female predominance in the pediatric group and is more commonly occurring at the craniocervical junction, with decreasing incidence caudally along the spine, in contrast to the craniocervical and sacrococcygeal predominance in the adult populations.[5]

EMBRYOLOGY AND HISTOPATHOLOGY

The notochord remnant is believed to be the precursor of chordomas. The notochord is a transient embryological structure that is established after gastrulation at the 3rd week of embryo development.[6] It is believed to promote the development of the neural tube and eventually regresses with its remnants developed into the nucleus pulposus of the intervertebral disks.[7]

It is believed that the activation and proliferation of notochord remnants give rise to the formation of chordomas.[6] It is proposed that the normal Brachyury mRNA expressing notochord cells could be transformed into the aberrant Brachyury mRNA expressing cells found in chordomas under different mechanisms, resulting in the formation of chordomas.[7] On the other hand, chordomas are hypothesized to arise from malignant transformation of the benign notochordal cell tumors.[8]

Macroscopically, chordomas are lobulated masses with a typical gelatinous or chondroid appearance. Microscopically, they are composed of cells embedding in a chondroid or myxoid stroma, giving the characteristic high T2-weighted hyperintense signal in magnetic resonance imaging (MRI). The hallmark of diagnosing chordomas is physaliphorous cells, which have abundant eosinophilic cytoplasm and intracytoplasmic vacuoles.[9]

Multiple immunohistochemical markers have been proposed such as cytokeratin, EMA, S100 and Brachyury. However, Brachyury becomes the principal marker for diagnosis since it is present in almost all chordomas but not found in chondrosarcomas.[9]

IMAGING FEATURES

General features

In general, chordomas present as midline, locally aggressive osteolytic lesions with associated soft-tissue masses on radiographs. Intratumoral calcifications may occasionally be depicted.

Computed tomography (CT) is used to evaluate the extent of the disease. Intratumoral calcifications could be better demonstrated. Chordomas show variable attenuations on CT but usually enhance after contrast injection.

Chordomas are further characterized in MRI. In general, T1-weighted, T2-weighted, and post-contrast studies are performed for characterization. Fat-saturated sequences may be applied to suppress the fat marrow signals for better delineation. They generally demonstrate low-to-intermediate T1-weighted signal with characteristic marked T2-weighted hyperintense signal due to the presence of vacuolated cellular components which contain high fluid contents. Small foci of hyperintense T1-weighted signal may be seen due to intratumoral hemorrhage or proteinaceous contents. T2 hypointense-weighted fibrous septa could also be seen. They usually show moderate enhancement after gadolinium injection, but occasionally only mild enhancement could be depicted if the tumor is relatively necrotic. On the other hand, complications including cord compression and invasion to the adjacent nerves and vascular structures could be illustrated.

Since chordomas are found at midline with locally aggressive features, vital neurovascular structures are always involved. If there is a suspicion of vascular encasement, CT and MR angiograms may be required to denote the patency of the arteries.

Chordomas may rarely metastasize to distant organs. Functional scans including bone scan and positron emission tomography (PET) may be used as part of the workup for the detection. However, for the primary tumors, they do not have clinical roles since they show variable uptakes.

Spheno-occipital

Cranial chordomas are usually found at the clivus and presented as a midline expansile soft-tissue mass with bone destruction on computed tomography studies [Figure 1a]. Irregular intratumoral calcifications could be seen,

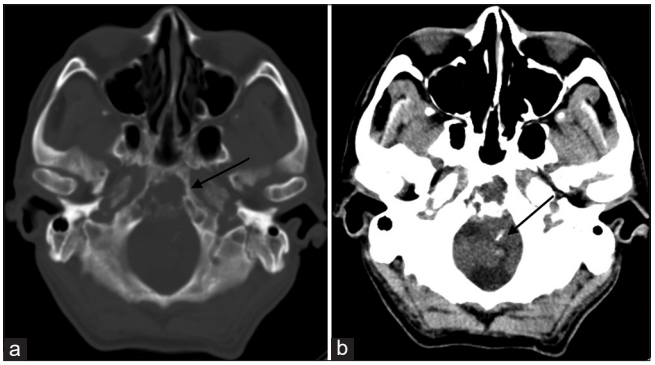

Figure 1: (a) Plain CT brain. Destructive clival mass involving the foramen magnum (black arrow). (b) Plain CT brain. The presence of intratumoral calcification. Extension of the mass into the foramen magnum with compression onto the medulla (black arrow).

representing sequestra from bone destruction [Figure 1b].[10] Enhancement of the lesion could often be demonstrated on post-contrast images.

MRI is the best modality to characterize cranial chordomas. They usually show a low-to-intermediate T1-weighted signal with a hyperintense T2-weighted signal [Figure 2a and b]. Small foci of T1-weighted hyperintensities may be evident if there is the presence of intratumoral hemorrhage or could be related to the proteinaceous mucinous content. Low T2-weighted fibrous septations are usually depicted. Heterogeneous enhancement with honeycombing appearance [Figure 2c][10] could be demonstrated after gadolinium injection.

Cranial chordomas could spread posteriorly to the foramen magnum, nasopharynx, and brainstem [Figure 2d]; inferiorly to the dens [Figure 2e]; laterally to the middle cranial fossae cavernous sinus [Figure 3a and b] and petrous apices; superiorly to the third ventricle and optic chiasm [Figure 3c]; anteriorly to the sella, sphenoidal, and ethmoid sinuses [Figure 4]; and inferolaterally to the pterygoid muscle [Figure 5a].

The patency of the internal carotid and basilar arteries could be assessed based on the presence of normal flow voids in the T2-weighted sequence, but is better evaluated on contrast MR angiography. Narrowing or occlusion of the arteries is rare despite encasement since chordomas are generally soft [Figure 5b].[10]

There are no characteristic spectroscopic findings.

Skull base chondrosarcomas are common mimickers of cranial chordomas. They share similar imaging features with chordomas. Diffusion weighted imaging might have a role to differentiate between the two but large-scale prospective studies are needed to determine the definite cutoff values.[11] For the location, since chondrosarcomas are believed to mesenchymal in origin, arise from the cartilage, bones with endochondral ossification, and primitive mesenchymal cells of the meninges, they are more likely to be centered laterally along the petro-occipital fissure in contrast to the midline location of chordomas.[12] Biopsy is still required currently for definite diagnosis.

Giant cell tumors of the skull base could be another differential diagnosis. However, they are more commonly found in the sphenoid bone and show a low-to-intermediate T2-weighted signal.[12] Skull base schwannoma may often have specific "target sign" appearance on T2-weighted images.[13]

Skull base metastases are the more common aggressive skull base lesions and should always be in the list of differential diagnoses when there is known primary malignancy.

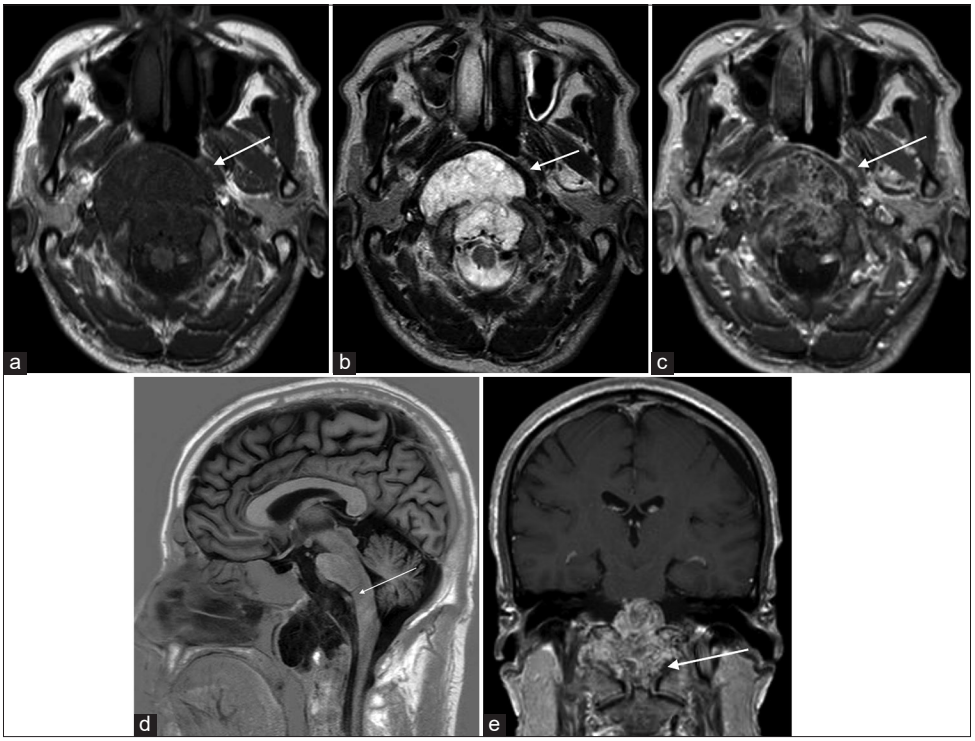

Figure 2: (a-c) Contrast MRI brain. A lobulated T1-weighted hypointense and T2-weighted hyperintense clival mass with moderate heterogeneous contrast enhancement, showing a honeycombing appearance (white arrows). (d) Contrast MRI brain. Extension of the mass into the foramen magnum with compression onto the brainstem. (e) Contrast MRI brain. Inferior extension with dens erosion (white arrows).

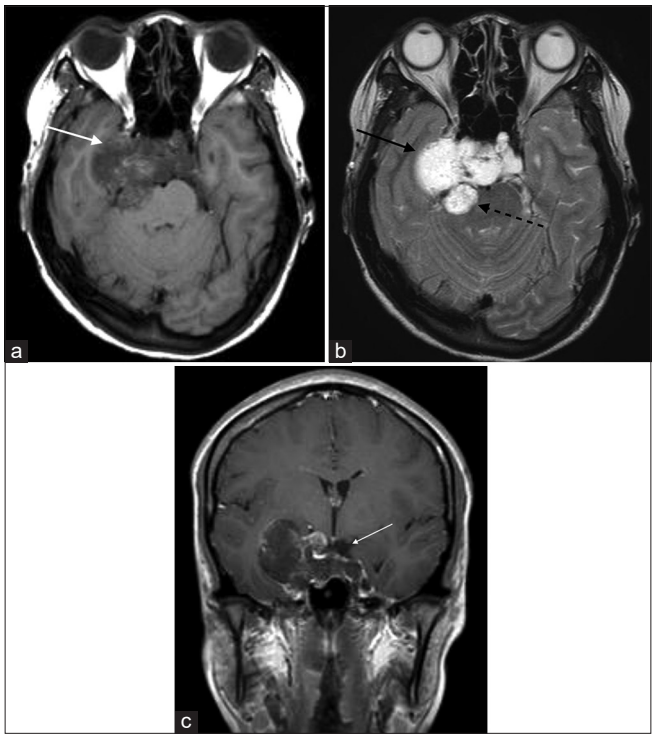

Figure 3: (a and b) Contrast MRI brain. Lateral extension of the mass into the right middle cranial fossa (white arrow), right cavernous sinus, and right petrous apex with compression onto the right mesial temporal lobe (black arrow). Posterior extension onto the midbrain was also evident (dotted black arrow). (c) Contrast MRI brain. Superior extension of the mass with compression on pituitary stalk and optic chiasm.

Figure 4: Plain CT brain. An lobulated mass centered at the right petroclival region (dark arrow) with extension into the right posterior ethmoid sinus and right sphenoid sinus (white arrow).

Vertebral bodies

Chordoma is a rare tumor of vertebral bodies by itself. However, it is the second most common primary spinal malignancy documented after lymphoproliferative disease.[14] If present, it is more commonly affecting the cervical spine, in particular at the upper cervical region than their thoracic and lumbar companions.[15]

On plain radiographs, chordoma is aggressive looking with lytic bony erosions and often associated with extraosseous soft-tissue swelling [Figure 6].

The anatomy and extent of the bony lesion could be delineated in CT studies. They are always used concomitantly with MRI to look for intratumoral calcifications [Figure 7a and b].

Local aggressiveness of the disease such as epidural involvement causing cord compression [Figure 7a], as well as involvement of neuroforamen [Figure 7c] encasement of the adjacent vasculatures, for instance vertebral arteries in cases of cervical spinal chordoma [Figure 8], could also be demonstrated.

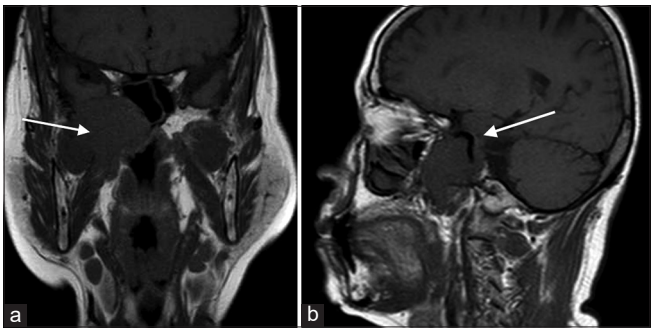

Figure 5: (a) Contrast MRI scan. Inferior extension into the right infratemporal fossa, abutting the pterygoid muscles (white arrow). (b) Contrast MRI scan. Encasement of the petrous and cavernous portion of the right internal carotid artery (white arrow).

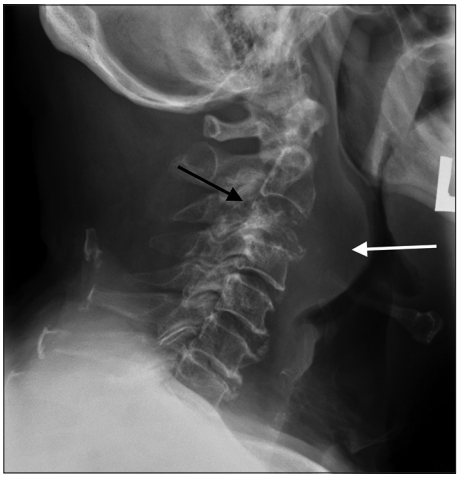

Figure 6: Lateral projection of cervical spine radiograph. Lytic cervical spine lesion at C3 level with partial vertebral collapse (black arrow). It was associated with prevertebral soft-tissue swelling spanning from C2 to C4 levels (white arrow).

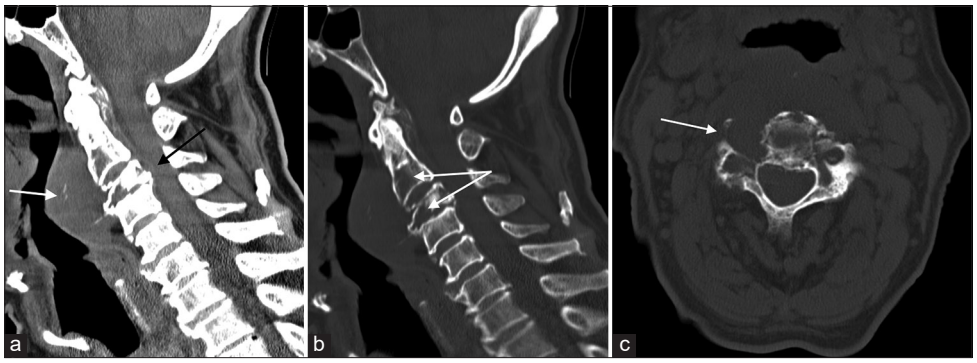

Figure 7: (a) Plain CT cervical spine. Cervical spine tumor at C2–C3 levels. It was associated with prevertebral soft-tissue mass spanning across C2–C4 levels with intratumoral calcifications within (white arrow). There was epidural involvement at the anterior epidural space (black arrow). (b) Plain CT cervical spine. Bone destruction at C2 and C3 vertebrae. (c) Plain CT cervical spine. Involvement of the right C3 neuroforamen.

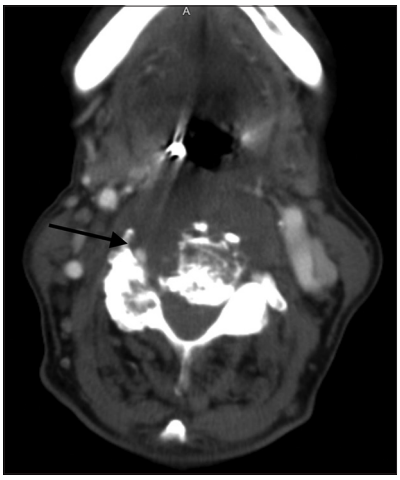

Figure 8: Contrast CT cervical spine. Encasement of the right vertebral artery which remained opacified (black arrow).

MRI aids the characterization of the lesion and potential complications including cord compression.

The soft-tissue masses of chordomas are characteristically spanning across several vertebral levels [Figure 9a-c].[15] They could spread anteriorly to the prevertebral levels or posteriorly involving the epidural space, demonstrating a draped curtain sign [Figure 9d]. There is characteristic sparing of intervertebral disk spaces.[15]

In the cervical region, chordomas could also enlarge the neuroforamen, giving a dumbbell appearance, and mimicking neurogenic tumors on axial images.[15]

Due to their local aggressiveness, chordomas could also encase or invade the adjacent vertebral arteries. The patency of the vertebral artery could be assessed by the preservation of flow void signals on MR studies [Figure 9d]. Angiograms would better assess their patency in equivocal cases.

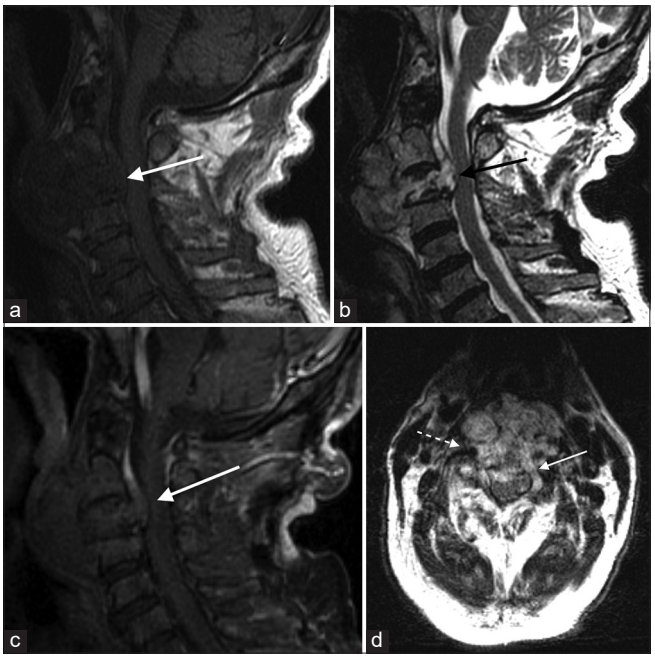

Figure 9: (a-c) MRI cervical spine. A T1-weighted hypointense and T2-weighted hyperintense cervical spine tumor with mild contrast enhancement. (d) The mass extended into and obliterated the anterior epidural space, demonstrating a draped curtain sign (white arrow). Normal T2-weighted flow void pattern of the right vertebral artery was preserved (dotted arrow).

Spinal chordomas may demonstrate an increase in SUV on PET [Figure 10]. However, in general, they do not have characteristic imaging features on functional studies.

Sacrococcygeal

Chordomas are the most common primary malignant tumors in the sacrum.[16] Due to their indolent nature, they are usually presented as a bulky, local aggressive pelvic mass at the time of diagnosis.

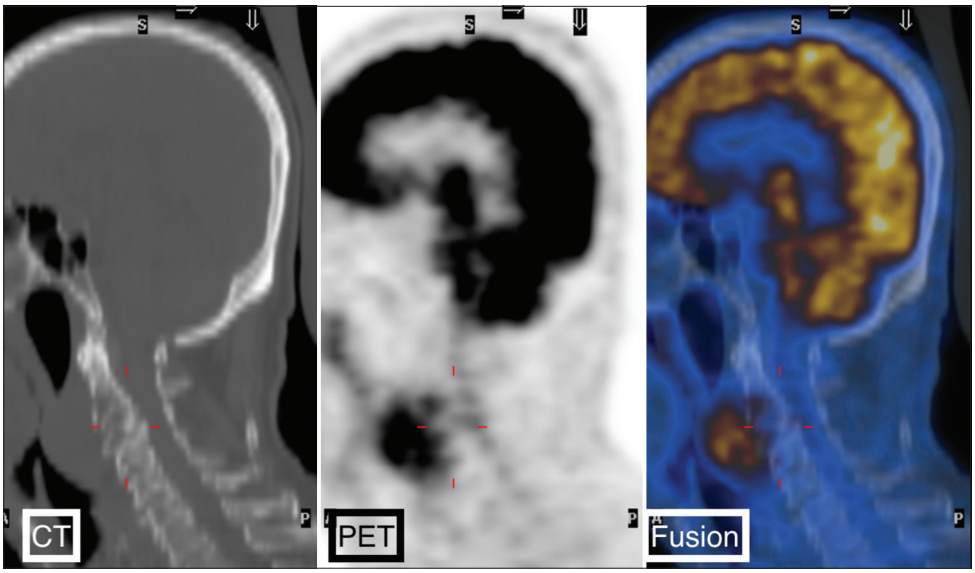

Figure 10: PET-CT scan. An increase in SUV (SUVmax 6.9) was demonstrated.

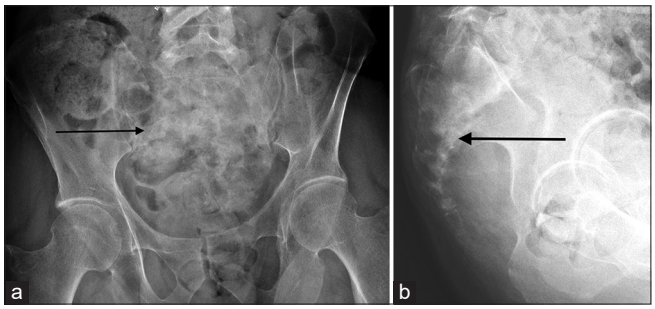

Figure 11: (a and b) Frontal and lateral radiographs of the sacrum. Destructive lytic lesion sacral lesion, with better demonstration on the lateral view (black arrows).

Frontal radiographs may have limited roles in the early stage of the disease since there is poor visualization of bony erosions at the sacrococcygeal regions due to overlapping colonic shadows in the pelvic region. Complementary lateral view would better demonstrate early erosive changes [Figure 11a and b].

In the late stage of the disease, destructive osteolytic lesions with the presence of presacral soft-tissue mass could be depicted on the radiographs.

CT studies are again used to evaluate the extent of the bony lesion and the presence of amorphous calcifications [Figure 12a-c].

Sacral chordomas usually grow within the sacrum, destroying the sacral foramina, and affecting the sacral nerve roots [Figure 13a-c].[17] They could also invade the greater sciatic foramen posteromedially and threaten the sciatic nerve. Laterally, they could grow across the sacroiliac joints and spread to the iliac bones [Figure 13d]. Posterolaterally, they could invade the pelvic muscles such as piriformis and

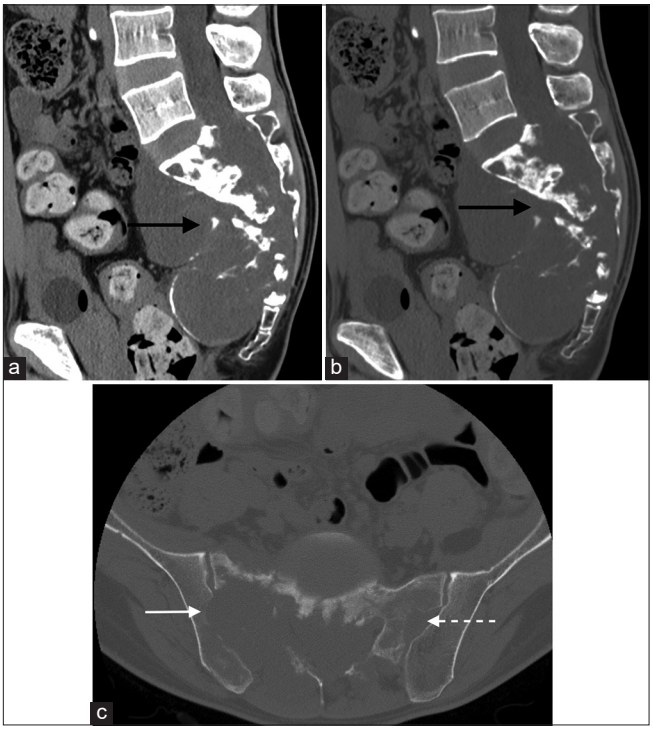

Figure 12: (a and b) Plain CT pelvis. Destructive sacral lytic lesion with soft-tissue mass containing intratumoral calcifications. (c) Plain CT pelvis. The mass eroded the right sacral foramen, extended across the right sacroiliac joint, and invaded the right iliac bone (white arrow). It also extended to the left sacroiliac joint (white dotted arrow).

gluteus maximus directly. Anteriorly, the mass could bulge into the mesorectum. However, invasion into the rectum is characteristically spared [Figure 14a-d] since the presacral fascia is tough and limits the spread of the disease.[18]

Figure 13: (a-c) Contrast MRI pelvis. A lobulated sacral mass with T1-weighted isointense and T2-weighted hyperintense signal showing mild contrast enhancement. (d) Contrast MRI pelvis. It invaded the right sacroiliac joint and the right ilium (white arrow). There was also involvement of the left sacroiliac joint (white dotted arrow).

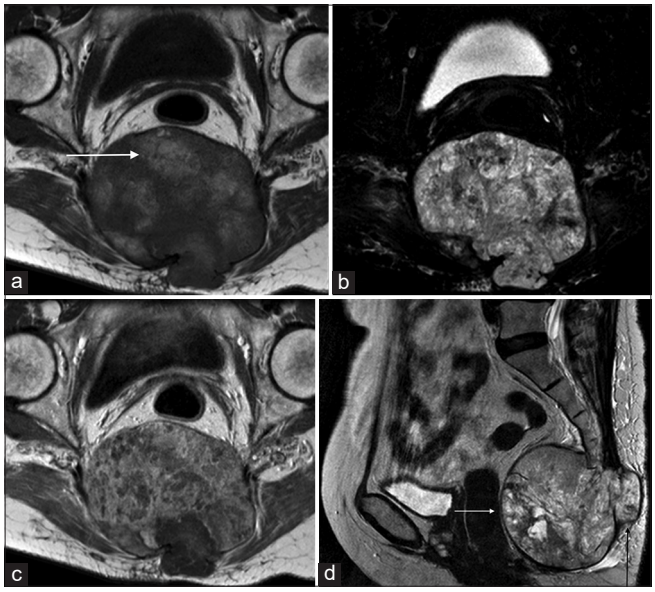

Figure 14: (a-c) Contrast MRI pelvis. Expansile pelvic mass centred at the sacrococcygeal junction showing a low to intermediate T1-weighted signal with presence of T1-weighted hyperintense foci indicating intralesional haemorrhage or proteinaceous contents high T2-weighted signal on fat-saturation images and moderate heterogeneous contrast enhancement. (d) Contrast MRI pelvis. Preserved intervening fat plane with the rectum anteriorly (white arrow). Focal breaching of tumour capsule invading into subcutaneous fat posteriorly (black arrow).

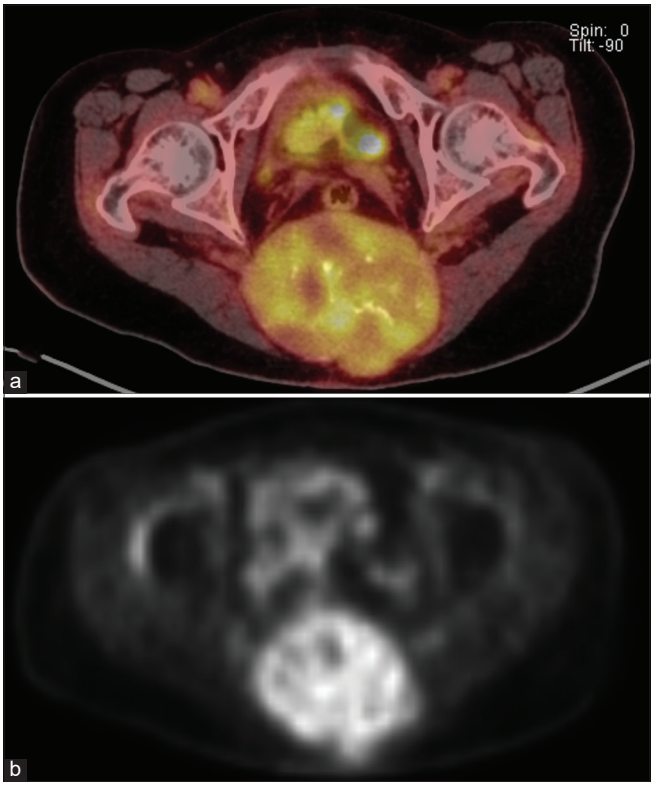

Figure 15: a and b PET-CT scan. An increase in uptake of the sacral tumour (SUVmax 6.7).

No characteristic imaging features could be seen in bone scans or PET. The scintigraphy uptake in bone scans or SUV values in PET scans can be variable [Figure 15a and b].

Other common differential diagnoses in the spine and sacrum include bone metastases, lymphoma, giant cell tumors, chondrosarcomas, and multiple myelomas.

There are variable appearances of spinal lymphoma, including lytic, mixed, and ivory vertebra. They usually do not show large areas of bone destruction, but are presented as a focus of bone marrow infiltration and soft-tissue mass.[14]

Giant cell tumors of the sacrum are the second most common primary tumors in the sacrum. They are usually eccentrically located and do not contain intratumoral calcifications. They usually affect younger populations with female predilection.[19] They may have coexisting secondary aneurysmal bone cysts with the presence of fluid-fluid levels.

Chondrosarcomas of the vertebral bodies could occur in the posterior elements, the vertebral bodies or both sites, sharing indistinguishable features with chordomas,[14] whereas chondrosarcomas of the sacrum are usually eccentrically located in the sacral ala and could also grow across the sacroiliac joint. There is characteristic septal and peripheral enhancement corresponding to the vascular septations.[19]

Multiple myelomas are usually presented as lytic bone lesions with a narrow zone of transition.[19] They do not have large soft-tissue components as in chordomas. Other sites of involvement are often seen in multicentric disease.

TREATMENT

The mainstay of treatment for chordomas is surgical resection. *En bloc* resection is preferred but often infeasible due to the local aggressiveness of the disease with invasion into the salient neurovascular structures, thus leading to high rate of disease recurrence due to tumor seeding.[20] Radiotherapy could be an option for local control of unresectable disease; however, it is challenging since chordomas are located in the midline of the axial skeletons with close relationships to vital neurovascular structures.[20]

Brachyury, a transcription factor which is present in almost all chordomas, is a new potential target that is still under clinical trials.[20,21]

CONCLUSION

Chordomas are rare, locally aggressive tumors at the midline structures arising from the notochord remnants. This pictorial essay discusses the common imaging features of cranial, spinal, and sacral chordomas. Differential diagnoses including chondrosarcoma and metastases should always be considered. Biopsy and multidisciplinary involvement are often required for definitive diagnosis and disease management.

Declaration of patient consent

Patients' consent not required as patients' identity is not disclosed or compromised.

Financial support and sponsorship

Nil.

Conflicts of interest

There are no conflicts of interest.

REFERENCES

1. Das P, Soni P, Jones J, Habboub G, Barnholtz-Sloan JS, Recinos PF, *et al.* Descriptive epidemiology of chordomas in the United States. J Neurooncol 2020;148:173-8.
2. Miller BJ. Population-based registries are important in sarcoma: An editorial regarding incidence patterns of primary bone cancer in Taiwan (2003-2010). Ann Surg Oncol 2014;21:2466-7.
3. Stacchiotti S, Sommer J, Chordoma Global Consensus Group. Building a global consensus approach to chordoma: A position paper from the medical and patient community. Lancet Oncol 2015;16:e71-83.
4. Bakker SH, Jacobs WC, Pondaag W, Gelderblom H, Nout RA, Dijkstra PD, *et al.* Chordoma: A systematic review of the epidemiology and clinical prognostic factors predicting progression-free and overall survival. Eur Spine J 2018;27: 3043-58.
5. Sebro R, DeLaney T, Hornicek F, Schwab J, Choy E, Nielsen GP, *et al.* Differences in sex distribution, anatomic location and MR imaging appearance of pediatric compared to adult chordomas. BMC Med Imaging 2016;16:53.
6. Ramesh T, Nagula SV, Tardieu GG, Saker E, Shoja M, Loukas M, *et al.* Update on the notochord including its embryology, molecular development, and pathology: A primer for the clinician. Cureus 2017;9:e1137.
7. Nibu Y, José-Edwards DS, Di Gregorio A. From notochord formation to hereditary chordoma: The many roles of Brachyury. Biomed Res Int 2013;2013:826435.
8. Sun X, Hornicek F, Schwab JH. Chordoma: An update on the pathophysiology and molecular mechanisms. Curr Rev Musculoskelet Med 2015;8:344-52.
9. Karpathiou G, Dumollard JM, Dridi M, Dal Col P, Barral FG, Boutonnat J, *et al*. Chordomas: A review with emphasis on their pathophysiology, pathology, molecular biology, and genetics. Pathol Res Pract 2020;216:153089.
10. Erdem E, Angtuaco EC, Van Hemert R, Park JS, Al-Mefty O. Comprehensive review of intracranial chordoma. Radiographics 2003;23:995-1009.
11. Yeom KW, Lober RM, Mobley BC, Harsh G, Vogel H, Allagio R, *et al.* Diffusion-weighted MRI: Distinction of skull base chordoma from chondrosarcoma. AJNR Am J Neuroradiol 2013;34:1056-61, S1.
12. Kunimatsu A, Kunimatsu N. Skull base tumors and tumor-like lesions: A pictorial review. Pol J Radiol 2017;82:398-409.
13. Skolnik AD, Loevner LA, Sampathu DM, Newman JG, Lee JY, Bagley LJ, *et al.* Cranial nerve schwannomas: Diagnostic imaging approach. Radiographics 2016;36:1463-77.
14. Rodallec MH, Feydy A, Larousserie F, Anract P, Campagna R, Babinet A, *et al*. Diagnostic imaging of solitary tumors of the spine: What to do and say. Radiographics 2008;28:1019-41.
15. Smolders D, Wang X, Drevelengas A, Vanhoenacker F, De Schepper AM. Value of MRI in the diagnosis of non-clival, non-sacral chordoma. Skeletal Radiol 2003;32:343-50.
16. Diel J, Ortiz O, Losada RA, Price DB, Hayt MW, Katz DS. The sacrum: Pathologic spectrum, multimodality imaging, and subspecialty approach. Radiographics 2001;21:83-104.
17. Hain KS, Pickhardt PJ, Lubner MG, Menias CO, Bhalla S. Presacral masses: Multimodality imaging of a multidisciplinary space. Radiographics 2013;33:1145-67.
18. Pillai S, Govender S. Sacral chordoma: A review of literature. J Orthop 2018;15:679-84.

19. Senne J, Nguyen V, Staner D, Stensby JD, Bhat AP. Demystifying sacral masses: A pictorial review. Indian J Radiol Imaging 2021;31:185-92.
20. Barber SM, Sadrameli SS, Lee JJ, Fridley JS, The BS, Oyelese AA, *et al*. Chordoma current understanding and modern treatment paradigms. J Clin Med 2021;10:1054.
21. Meng T, Jin J, Jiang C, Huang R, Yin H, Song D, *et al.* Molecular targeted therapy in the treatment of chordoma: A systematic review. Front Oncol 2019;9:30.

How to cite this article: Lee SH, Kwok KY, Wong SM, Chan CX, Wong YT, Tsang ML. Chordoma at the skull base, spine, and sacrum: A pictorial essay. J Clin Imaging Sci 2022;12:44.